Intentional mistuning optimization of nonlinear mistuned bladed-disks.

E. CAPIEZ-LERNOUT[a], C.SOIZE[b]

a. E. Capiez-Lernout, Université Gustave Eiffel, MSME UMR 8208 CNRS, 5 bd Descartes, 77454 Marne-la-Vallée, France, evangeline.capiez-lernout@univ-eiffel.fr
b. C. Soize, Université Gustave Eiffel, MSME UMR 8208 CNRS, 5 bd Descartes, 77454 Marne-la-Vallée, France, christian.soize@univ-eiffel.fr

Abstract :

One major industrial challenge is to consider the detuning as a technological means to reduce the dynamical amplifications induced by mistuning. A full analysis of the detuning optimization of mistuned bladed-disks with finite displacements is carried out on a 12 bladed-disk finite element model. The paper is based on a computational methodology previously developed by the authors. We then have to be very careful with the construction of an adapted scalar quantity of interest for defining the detuning optimization problem. Direct computations allowing for all possible detuned configurations to be considered allow for obtaining a full data basis. A meticulous post-processing shows the existence of a few detuned configurations, that inhibits the mistuning amplification effects of the pure mistuned bladed-disk.

Keywords : intentional mistuning - detuning, mistuning, geometrical nonlinearities, optimization

1 Introduction :

The vibrational behavior of turbomachines is known to be particularly complex. More particularly, the mistuning phenomenon caused by the small variations of the mechanical properties or by the manufacturing tolerances from one sector to another one can generate strong localization effects yielding subsequent dynamical amplifications of the forced response with respect to the perfect cyclic symmetry. The intentional mistuning, also called detuning, consists in voluntarily breaking the cyclic symmetry of the structure by using partial or alternating patterns of different sector types. The detuning allows for spreading the frequencies of adjacent blades and thus for reducing the interaction between them. The manuscript presents a numerical validation concerning the detuning optimization of a mistuned 12 bladed-disk structure in presence of geometrical nonlinearities. The theoretical background that concerns the formulation, the methodology, the computational model including the construction of the NL-SROM (NonLinear Stochastic Reduced-Order Model) and the use of the nonparametric probabilistic approach for the mistuning modeling [2, 1] and all the dedicated algorithms can be found in [4, 3]. The computational analysis of a full data basis constituted of the set of all possible detuned configurations using a representative computational model of a 12-bladed-disk structure is carried out. The post-processing analysis then allows for constructing the exact solution of the detuning optimization problem.

2 Direct problem

2.1 Description of the computational model

The structure under consideration is a blisk with order $N = 12$ and with $n_w = N = 12$ blades whose finite element computational model is constructed with hexahedral solid finite elements with 8 nodes. The finite element mesh is issued from [5] for which the order of the cyclic symmetry has been modified from 24 to 12 as also used in [6]. The main motivation of such reduction of the number of blades is to decrease the number of possible detuning patterns in order to have a reasonable number of detuning possibilities, as previously explained. In the present case, the aim is to constitute a full reference data basis in the nonlinear mistuned/detuned context. Indeed, when the detuning concept is approached with 2 possible types of blades, there are 352 possible detuned configurations when $N = 12$ that reduces the number of possibilities by a factor of almost $2^{N-1} \simeq 2\,000$ with respect to a structure with cyclic symmetry of order $2N = 24$. Let $(0, \mathbf{X}, \mathbf{Y}, \mathbf{Z})$ be the Cartesian reference coordinate system for which $(0, \mathbf{Z})$ coincides with the rotational axis for the blisk. Fig. 1 shows the finite element mesh of the blisk whose computational characteristics are summarized in Table 1. There are $n = 27\,108$ degrees of freedom (dof). The blisk is made up of a homogeneous and isotropic material with mass density $7\,860\, Kg/m^3$, Poisson ratio 0.25, and Young modulus $2{\times}10^{11} N/m^2$. A Dirichlet condition is applied along the interfaces toward adjacent stages [5]. The fundamental frequency of the blisk is $\nu_0 = 977.32\, Hz$. A Rayleigh damping model is added for the blisk, with parameters $\alpha = 78.67\, s^{-1}$ and $\beta = 3.69 \times 10^{-7}\, s$ chosen such that the critical damping rate $\xi(2\pi\nu)$ belongs to $[0.0054, 0.008]$ for $\nu \in [900\,, 6\,000]\, Hz$.

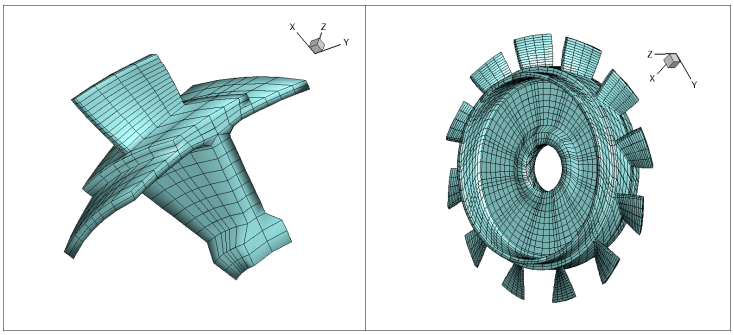


FIGURE 1 – Finite element mesh of the blisk : blade sector (left figure), full blisk (right figure)

	Elements	Nodes	dof
Sector	476	846	2151
Full model	5712	9 036	27 108

TABLE 1 – Computational characteristics of the finite element model

Since we are interested in the forced response of the structure, the presence of geometrical nonlinearities requires to solve the nonlinear dynamical equations in the time domain. The external loading is defined in order to excite uniformly all frequencies located in $\mathbb{B}_e = [4700, 5200]\, Hz$ where there is a veering corresponding to $h = 2$ nodal diameters occuring et eigenfrequencies $\nu_{2,4} = 4\,845.18\, Hz$ (dominant blade motion) and to eigenfrequency $\nu_{2,5} = 5\,091.09\, Hz$ (blisk global motion).

Each detuned configuration of the blisk in presence of random mistuning is modeled by a nonlinear stochastic reduced-order model (NL-SROM) whose methodology of construction is not given in this paper.

For a given detuned configuration, the NL-SROM is obtained from the finite element model, for which the physical displacements are projected on a vector basis [4, 3] that allows for obtaining a deterministic nonlinear reduced-order model. The mistuning is assumed to only affect the linear elastic internal force and the nonlinear forces, which are therefore uncertain. Note that the nonlinear internal forces are directly evaluated in the reduced space, by direct numerical evaluation from the finite element model. Uncertainties are implemented from the deterministic nonlinear reduced-order model using the nonparametric probabilistic approach [2, 1]. All the numerical parameters that are involved in the construction of the nonlinear mistuned forced response of the blisk are optimized.

2.2 Observation of interest for the direct problem

The computational model of the detuned blisk is constructed from the knowledge of two identical meshes of two different sector types denoted as 1 and 2. The reference sector 2 is obtained from sector 1 by decreasing the Young modulus of the blade from $\mathrm{Young}_1 = 2.00\times10^{11}\,\mathrm{N/m^2}$ to $\mathrm{Young}_2 = 1.80\times10^{11}\,\mathrm{N/m^2}$. For the tuned blisk with cyclic symmetry of order $N = 12$, there are a total number of $n_c = 352$ possible detuned configurations. The detuned configuration in presence of mistuning is defined by a given distribution of the blades of type 1 and 2. The detuned configuration number ℓ is then represented by a vector $\mathbf{w}^{c,\ell} \in \{0,1\}^{n_w}$ whose component $w_j^{c,\ell}$ is equal to 0 or 1 whether the blade is of type 1 or of type 2. The objective is to find detuned configurations whose mistuning effects induce less amplification than the one obtained with the tuned configuration in presence of mistuning. The idea is then to define a scalar quantity that is able to quantify the mistuning effects of the detuned configuration with respect to the unavoidable mistuning effects of the tuned configuration. We define the scalar observation $a^{\ell,k}$ such that $a^{\ell,k} = \max_j\{\max_i \|\mathbf{X}^\ell(j,2\pi\nu_i,\theta_k)\|\}$ .in which $\mathbf{X}^\ell(j,2\pi\nu_i,\theta_k)$ the $\mathbb{C}^{3n_b}$-vector of the realization θ_k of the $3n_b$-displacement dofs of blade number $j \in \{1,\ldots,n_w\}$ in the frequency domain, taken at frequency ν_i, and corresponding to the detuned configuration number ℓ. In order to get a robust scalar quantity for characterizing the random nonlinear dynamical behavior of the blisk, an estimate of the maximum extreme value statistics of random variable A^ℓ is constructed as follows. The available number of Monte Carlo numerical simulations is written as $n_{\mathrm{sim}} = \nu_r\,\nu_e$ (for $n_{\mathrm{sim}} = 500$, $\nu_e = 10$ and $\nu_r = 50$). We then define for $r \in \{1,\ldots,\nu_r\}$ quantity $\underline{a}_M^\ell$, such that $\underline{a}_M^\ell = \dfrac{1}{\nu_r}\displaystyle\sum_{r=1}^{\nu_r} a_M^{\ell,r}$ with $a_M^{\ell,r} = \max_{k\in\{\nu_e(r-1)+1,\ldots,r\nu_e\}} a^{\ell,k}$ .The observation of the detuned ℓ-configuration with mistuning is then defined as the amplification factor $q^{c,\ell}$ with respect to its tuned counterpart with pure mistuning, that is written as $q^{c,\ell} = \underline{a}_M^\ell/\underline{a}_M^{\mathrm{t}}$,in which superscript t is related to the tuned configuration. This subset corresponds to $n_c = 216$ possible detuned configurations for which the number nb_2 of blades of type 2 is less than or equal to $n_w/2 = 6$. From now on, only detuned configurations corresponding to $n_c = 216$ possible detuned configurations will be considered, assuming that the number nb_2 of blades of type 2 is less than or equal to $n_w/2 = 6$. Figure 3 summarizes the results obtained with these improving detuned configurations.

3 Nonlinear analysis of the mistuned response of the best and the worst detuned configurations

The results are analyzed for the following detuned configurations : the tuned configuration corresponding to the pure mistuning case ($\ell = 49$), the best detuned configuration ($\ell = 104$), and the worst detuned configuration ($\ell = 9$). Fig. 4 displays the graphs of $k \mapsto a^{\ell,k} = A^\ell(\theta_k)$ for $k = 1,\ldots,n_{\mathrm{sim}}$, which

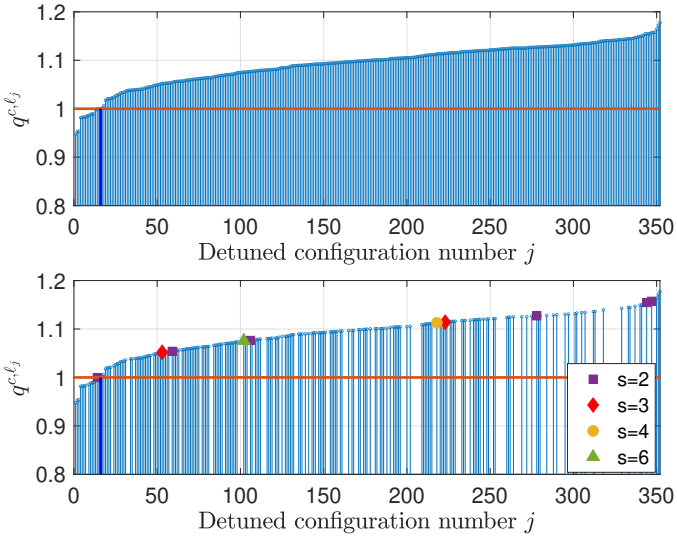


FIGURE 2 – Dynamical amplification factor according to detuned configuration. Graph of function $j \mapsto q^{c,\ell_j}$ for the $n_c = 352$ possible detuned configurations (upper graph) and for the $n_c = 216$ detuned configurations with a number of blades with type 2 less than or equal to 6 (lower graph). Subcyclicity order s is given for $s = 2$ (purple square symbol), $s = 3$ (red diamond symbol), $s = 4$ (orange bullet symbol) and $s = 6$ (green triangle symbol).

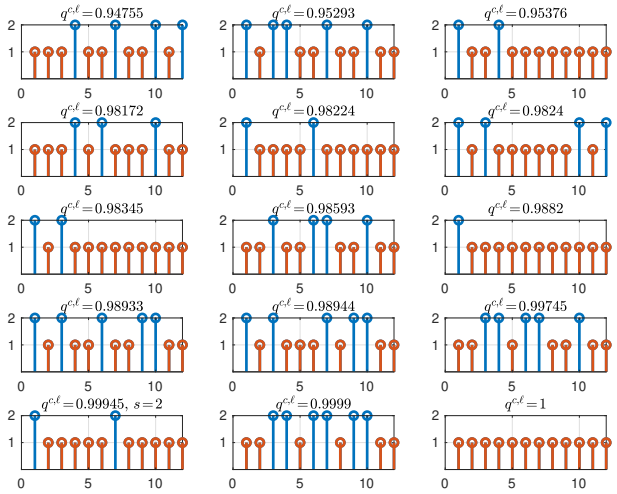


FIGURE 3 – Characteristics of the improving detuned configurations.

describes the maximum displacement response over the frequency and the blades for each mistuning realization θ_k of the detuned configurations $\ell \in \{49, 104, 9\}$. By comparing these graphs, it can be seen that the best detuned configuration is characterized by slightly lower response levels but also by less scattered realizations with respect to the pure mistuned case (left figure). The realizations of the worst detuned configurations (right graph) are clearly more scattered with higher response levels.

Furthermore, let $z^{\ell,+}_{\max}(2\pi\nu)$ be the upper bound of confidence region $Y^{\ell}_{\max}(2\pi\nu)$ normalized with respect to its pure mistuned counterpart. Figure 5 shows the graphs of $\nu \mapsto z^{\ell,+}_{\max}(2\pi\nu)$ for the 15 best and for the 15 worst detuning configurations. It can be seen that the first resonance that is also the main resonance of the pure mistuned system is the one that is involved in the detuning optimization process, the two other ones being robust to detuning optimization. To the contrary, the worst detuned configurations

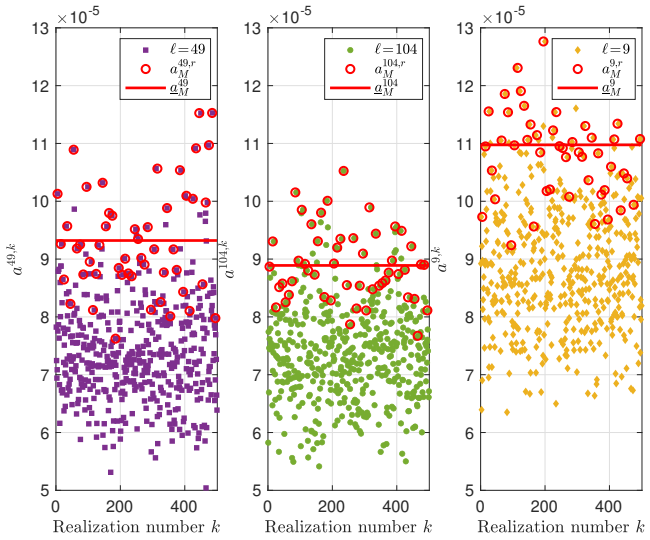


FIGURE 4 – Analysis of the mistuned response for given detuned configurations : graph of realizations $k \mapsto a^{\ell,k} = A^{\ell}(\theta_k)$ (colored symbols), of realizations $(5r+10) \mapsto a_M^{r,\ell}$ (red circle) and value of constant $\underline{a}_M^{\ell}$ (red thick line) for the tuned configuration (pure mistuning) $\ell = 49$ (left figure), the best detuned configuration $\ell = 104$ (middle figure), and the worst detuned configuration $\ell = 9$ (right figure).

violate the critical level through the two first resonances. All these observations allow for assessing the efficiency of the optimization through the output of interest $q^{c,\ell}$.

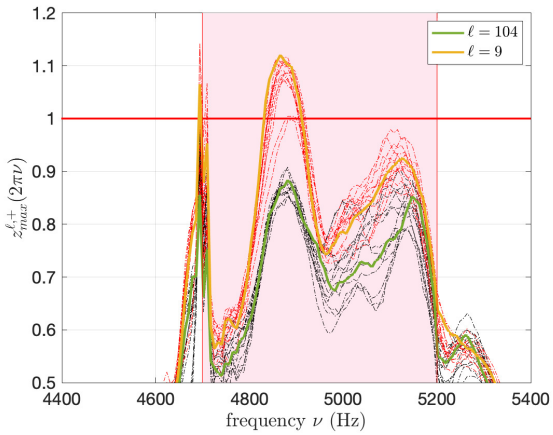


FIGURE 5 – Analysis of the mistuned response for given detuned configurations : zoom of the upper bound of confidence region $\nu \mapsto z_{\max}^{\ell,+}(2\pi\nu)$ for the best detuned configuration $\ell = 104$ (green line), for the worst detuned configuration $\ell = 9$ (orange line), for the 15 best configurations (black dashed-dotted lines) and for the 15 worst configurations (red dashed-dotted lines). Critical level corresponding to the pure mistuned situation is set to 1 (red line).

4 Conclusion

We have presented an application allowing for the optimization of the detuning in presence of random mistuning and geometrical nonlinearities for bladed disks, based on the use of high-fidelity computational models.

A particular attention concerns the choice of the observation chosen in the formulation of the detuning optimization problem. It is found that there is a few number of optimal solutions with respect to the number of possible detuned configurations. It is also proved that the optimization problem is well-posed, yielding to robust optimal detuned configurations that are identified after post-processing analysis as detuned configurations for which the mistuning amplification effects are inhibited with respect to the pure mistuning situation.

The detuning patterns yielding the best optimal detuned configurations and yielding the worst amplification response levels have no particularly structure in terms of number of blades of different types and of blade distribution, which deserve further investigations to understand the complex mechanisms induced by the detuning.

The availability of this full detuning data basis can also be viewed as a way to validate further optimization methodologies, by investigating the detuning optimization problem as a combinatorial optimization problem based on a probabilistic learning approach [7].

Acknowledgements

The authors thank Pr. Christophe Pierre from the Stevens Institute of Technology concerning the use of the bladed-disk finite element model.

Références

[1] M.-P. Mignolet, C. Soize, Stochastic reduced order models for uncertain geometrically nonlinear dynamical systems, Computer Methods in Applied Mechanics and Engineering 197 (45-48) (2008) 3951–3963.

[2] C. Soize, A nonparametric model of random uncertainties for reduced matrix models in structural dynamics, Probabilistic Engineering Mechanics 15 (3) (2000) 277–294.

[3] A. Picou, E. Capiez-Lernout, C. Soize, M. Mbaye, Robust dynamic analysis of detuned-mistuned rotating bladed disks with geometric nonlinearities, Computational Mechanics 65 (3) (2020) 711–730.

[4] E. Capiez-Lernout, C. Soize, M. Mbaye, Mistuning analysis and uncertainty quantification of an industrial bladed disk with geometrical nonlinearity, Journal of Sound and Vibration 356 (10) (2015) 124–143.

[5] R. Bladh, M. Castanier, C. Pierre, Component-mode-based reduced order modeling techniques for mistuned bladed disks. part 2 : application, ASME Journal of Engineering for Gas Turbines and Power 123 (1) (2001) 100–108.

[6] Y. Han, R. Murthy, M. Mignolet, J. Lentz, Optimization of intentional mistuning patterns for the mitigation of the effects of random mistuning, ASME Journal of Engineering for Gas Turbines and Power 136 (06) (2014) 062505.

[7] E. Capiez-Lernout, C. Soize, Nonlinear stochastic dynamics of detuned bladed-disks with uncertain mistuning and detuning optimization using a probabilistic machine learning tool, International Journal of Non-Linear Mechanics, 143(07) 104023, 2022.